Journal of Catalysis **204,** 305–313 (2001)
doi:10.1006/jcat.2001.3388, available online at http://www.idealibrary.com on IDEAL®

Lanthanide Oxide Doped Titanium Dioxide Photocatalysts: Effective Photocatalysts for the Enhanced Degradation of Salicylic Acid and *t*-Cinnamic Acid

K. T. Ranjit,*,[1] I. Willner,* S. H. Bossmann,† and A. M. Braun†

*Institute of Chemistry and Farkas Center for Light-Induced Processes, The Hebrew University of Jerusalem, Jerusalem, 91904, Israel; and †Lehrstuhl für Umweltmesstechnik der Universität Karlsruhe (TH), Engler-Bunte-Institut, Richard-Willstätter-Allee 5, 76128 Karlsruhe, Germany

Received February 26, 2001; revised August 10, 2001; accepted August 10, 2001; published online October 25, 2001

The photocatalytic degradation of salicylic acid and *t*-cinnamic acid has been investigated in aqueous suspensions of lanthanide oxide doped TiO_2 photocatalysts. Complete mineralization has been achieved in the case of lanthanide oxide doped TiO_2 photocatalysts in total contrast to the formation of intermediates in case of nonmodified TiO_2. The equilibrium dark adsorption of salicylic acid and *t*-cinnamic acid is ca. three times and two times higher, respectively, on the lanthanide oxide modified catalysts as compared to the nonmodified TiO_2 catalyst. The adsorption isotherms were analyzed in terms of the Langmuir theory and a good fit was obtained. The enhanced degradation is attributed to the formation of the Lewis acid–base complex between the lanthanide ion and the substrates at the photocatalyst surface. The concentration of the organic acids at the composite Ln_2O_3/TiO_2 photocatalysts could provide a means for the enhanced activity.

Key Words: **lanthanide oxide; doped titanium dioxide; photocatalyst; salicylic acid; *t*-cinnamic acid; adsorption.**

INTRODUCTION

The study of light-induced reactions catalyzed by semiconductors has been widely studied particularly during the past decade (1–5). A wide range of organic compounds such as phenols, aromatic carboxylic acids, dyes, surfactants, and pesticides have been successfully mineralized (6–10). Photocatalysis has also proven useful in the reductive deposition of heavy and noble metal ions like Pt^{4+}, Au^{3+}, Rh^{3+}, Cr^{3+}, etc. from aqueous solutions to surfaces (11–14). Among the several semiconductors employed for the degradation of organic compounds, TiO_2 has proven to be a versatile catalyst for detoxification of organic pollutants. The excellent stability coupled with low cost has made TiO_2 a benchmark catalyst in semiconductor photocatalysis. In order to effectively compete with e^-/h^+ recombination and trap effectively the conduction band electrons or the valence band holes, the respective electron acceptor or donor should be confined to the semiconductor surface. Several methods have been suggested to control the interfacial electron transfer at the semiconductor–electrolyte interface. These include encapsulation of electron acceptors on receptor functionalized semiconductors, (15) immobilization of semiconductor photocatalysts in redox functionalized polymers, (16) and electrostatic association of electron acceptors at the semiconductor surface (17).

Another method to improve the degradation is to preconcentrate the organic substrate at the semiconductor surface in order to effectively trap the respective reactive radicals. Concentration of the organic pollutant at the semiconductor surface has been achieved by selective doping of the semiconductor, (18) surface modification of the photocatalyst with chelating agents, (19) and surface modification of the catalyst with electron acceptors groups (20).

Lanthanide ions are known for their ability to form complexes with various Lewis bases (e.g., acids, amines, aldehydes, alcohols, thiols, etc.) in the interaction of these functional groups with the *f* orbitals of the lanthanides (21). Thus, incorporation of lanthanide ions in a TiO_2 matrix could provide a means to concentrate the organic pollutant at the semiconductor surface. The sol–gel method enables the synthesis of a high surface area TiO_2 particle (22). Here we wish to report on the degradation of salicylic acid and *t*-cinnamic acid on lanthanide oxide doped TiO_2 particles. The choice of salicylic acid as the substrate was based on the fact that it is well documented that aromatic carboxylic acids such as salicylic acid have great affinity for aqueous Ti(IV) and a strong tendency to chemisorb (24–26). Thus, it is important to assess if the activity of lanthanide oxide doped TiO_2 extends to the degradation of salicylic acid.

The photocatalytic degradation of salicylic acid has been the subject of numerous investigations. Matthews has studied the kinetics and the photocatalytic oxidation of salicylic acid on TiO_2 thin films, and a reaction mechanism involving peroxyhydroxycyclohexadienyl- and

[1] To whom correspondence should be addressed. Current Address: Department of Chemistry, The University of Houston, Houston, Texas 77204-5641. Fax: (713) 743-2709. E-mail: rkoodali@jetson.uh.edu.

0021-9517/01 $35.00

mucondialdehyde-type compounds as intermediates was proposed (27–31). Titanium dioxide aerogels, cryogels, and nanofibrils were also evaluated for the degradation of salicylic acid in aqueous environments (32–34).

EXPERIMENTAL

The nonmodified TiO_2, europium (Eu^{3+}), praseodymium (Pr^{3+}), and ytterbium (Yb^{3+}) doped TiO_2 were prepared as shown in Scheme 1. The preparation of these catalysts has been reported previously (18). The molar ratio of Ti(IV) to Eu(III), Pr(III), or Yb(III) is usually 100, but a catalyst having a molar ratio of Ti(IV) to Eu(III) corresponding to Ti/Eu = 20 was also prepared. The X-ray diffractograms of the calcined samples were recorded using a Philips PW 1050 powder diffractometer. The diffraction patterns were recorded at room temperature using a Ni-filtered Cu$K\alpha$ radiation ($\lambda = 1.5418$ Å) for the samples. Surface area measurements were measured by nitrogen adsorption at −196°C by the dynamic BET method using a Micromeritics II 2370 surface area analyzer. The transmission electron micrographs (TEM) of the samples were recorded using a JEOL, JEM-100 CX, electron microscope, operating at an accelerating voltage of 80 kV. X-ray photoelectron spectroscopy (XPS) analyses were performed with an AXIS-HS Kratos instrument using a monochromatized Al($K\alpha$) source ($h\nu = 1486.6$ eV). A flood gun was used to neutralize the sample surface, while the C (1s) line was used for a final energy scale calibration.

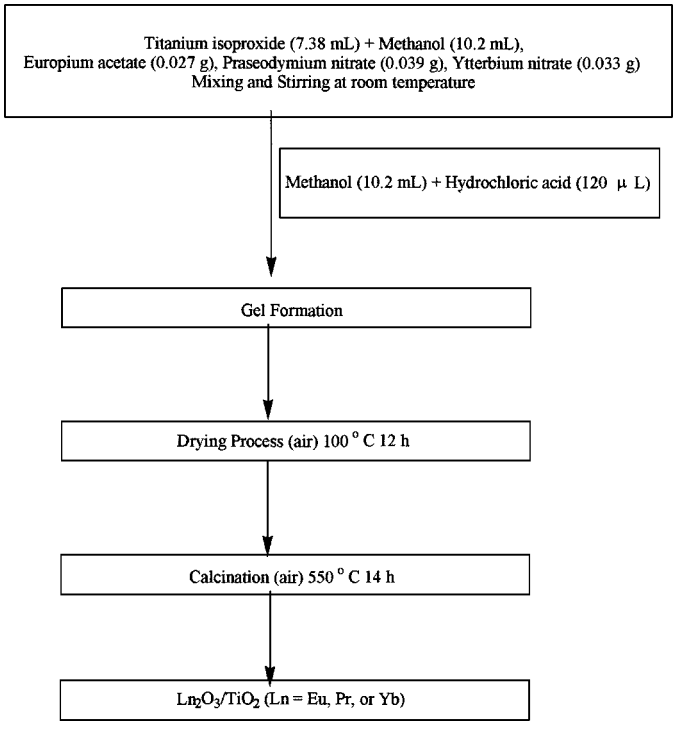

SCHEME 1. Preparation of the lanthanide oxide doped TiO_2 catalysts.

Adsorption of the organic substrate onto the catalysts was examined by stirring 2.5 mg of the catalyst in 2.5 ml of appropriate concentrations of the substrates in the dark. After equilibration for 1 h, the catalyst was filtered using a 0.05-μm polycarbonate filter and the concentration of the organic substrate was determined spectroscopically. The concentrations of salicylic acid and *t*-cinnamic acid before and after adsorption were measured from their absorption maximum at $\lambda = 295$ nm and $\lambda = 272$ nm, respectively. Photochemical degradation of salicylic acid and *t*-cinnamic acid was examined. The aqueous solution of the pollutant (2.5 mL), 2.4×10^{-4} M (salicylic acid) or 2.2×10^{-5} M (*t*-cinnamic acid), and 2.0–2.4 mg of the respective photocatalysts were placed in a quartz cuvette (5-mL capacity). The suspension was irradiated with a 200-W Xe(Hg) lamp (Oriel) equipped with an $CuSO_4$ solution to filter IR radiation. The flux of photons entering the reactor was $\sim 6 \times 10^{-6}$ einsteins/s in the 300- to 400-nm-wavelength range. A Pyrex filter was used to filter the light of wavelengths less than 300 nm that would cause direct photodegradation of the organic substrates. During irradiation, the suspension was stirred continuously and purged with oxygen. Oxygen bubbling throughout the experiment maintained a dissolved oxygen concentration of $\sim 1 \times 10^{-4}$ mol dm^{-3}. After irradiation, the suspension was filtered to remove the catalyst and the solution was analyzed spectroscopically (Uvikon-860 Kontron Spectrophotometer) and by gas chromatography–mass spectrometry/Fourier transform infrared spectroscopy (GC–MS/FTIR).

The light absorbed by the particles was determined by placing a radiometer at the back side of the quartz cuvette which contains the organic substrate solution alone or the same solution containing 2.0–2.4 mg of the modified TiO_2 particles. The difference between the two recorded values was assumed to correspond to the absorbed light intensity. Since light scattering by the particles is neglected, the absorbed light intensities could be considered as upper limits.

DOC Analyses

The analysis of dissolved organic carbon (DOC) was carried out using a Dohrmann DC-190 total organic carbon (TOC) analyzer ($T = 680$°C) from Rosemount Analytical. The organic components were oxidized in an oxygen atmosphere at a platinum/alumina contact. The amount of carbon dioxide formed was measured using a nondispersive IR detector. The TOC content was analyzed in this manner and the inorganic carbon content was subtracted from this value. The latter is obtained by treating the samples with concentrated phosphoric acid. The calibration was performed using salicylic acid, oxalic acid, and potassium hydrophthalate (KHP). All calibration samples could be

fitted with a linear calibration curve. The samples were injected three consecutive times (injection volume 50 μl) and the average values were reported.

GC–MS/FTIR Analysis

For the quantitative and qualitative analysis of the reaction products generated during the photolysis experiments, the samples (2 μl) were injected into a GC (HP 5971A MSD, mass selective detector) coupled with a HP 5965B 1D (infrared detector). A HP-INNOWAX capillary column (cross-linked polyethylene glycol) was employed. All reaction products were identified by a combination of MS and FTIR spectroscopy in comparison with analytical databases.

RESULTS AND DISCUSSION

Table 1 shows the physical properties of the TiO_2 catalysts prepared in the present study. The X-ray diffractograms of the samples reveal that in the case of the nonmodified TiO_2, the anatase phase is the major constituent of the photocatalyst (80%) accompanied by a rutile phase (20%). In the case of Eu_2O_3/TiO_2 and Yb_2O_3/TiO_2 the anatase phase is predominant (>95%), while in the case of Pr_2O_3/TiO_2 catalyst, the X-ray diffractogram reveals the presence of only the anatase phase. XPS measurements reveal that the lanthanide does exist in the resulting TiO_2 photocatalysts as oxides, Ln_2O_3. Lanthanide concentrations were evaluated from their 3d and 4d lines. The europium-doped TiO_2 photocatalysts, having a molar ratio of Ti/Eu = 20 and Ti/Eu = 100, show a characteristic band at 1134.7 eV due to the Eu^{3+} ion. The band characteristic of Ti^{4+} appears at 458.6 eV. The ratio of atomic concentration of Ti/Eu in the doped Eu_2O_3/TiO_2(starting molar composition Ti/Eu = 20) at the surface was evaluated to be 20 ± 2, in full agreement with the molar ratio of the ions used in the preparation of the photocatalyst prior to the calcination. However, for the catalyst Eu_2O_3/TiO_2 (starting molar composition Ti/Eu = 100), the ratio of the Ti/Eu at the surface was evaluated to be $\sim 40 \pm 4$ from XPS studies. Thus,

TABLE 1

Physical Properties of TiO_2 Photocatalysts

Catalyst	Phases	Surface area ($m^2\ g^{-1}$)	Particle size (nm)
TiO_2	Anatase (80%) Rutile (20%)	78	40–80
Eu_2O_3/TiO_2 (Ti/Eu = 20)	Anatase > (95%)	90	30–50
Eu_2O_3/TiO_2 (Ti/Eu = 100)	Anatase > (95%)	102	30–50
Pr_2O_3/TiO_2	Only anatase	125	25–40
Yb_2O_3/TiO_2	Anatase > (95%)	55	40–80

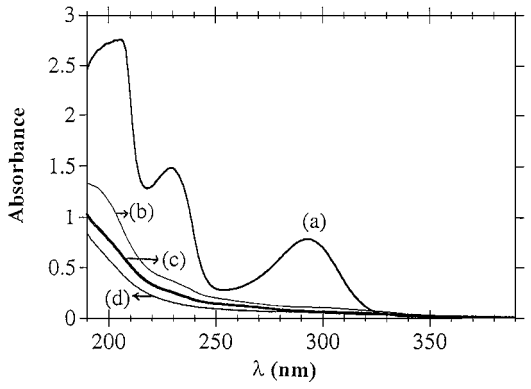

FIG. 1. Absorption spectra of an aqueous solution of salicylic acid (2.4×10^{-4} M) (a) before irradiation, (b) after 30 min of irradiation, (c) after 45 min of irradiation, and (d) after 60 min of irradiation in the presence of the Eu_2O_3/TiO_2 catalyst (Ti/Eu = 20) (2.4 mg in 2.5 ml of the solution).

there seems to be an enrichment of Eu^{3+} ion at the surface due to segregation of Eu_2O_3 to the surface after calcination. An additional Eu signal around 1125 eV was observed in the Eu_2O_3/TiO_2 samples, associated with the reduced form of the europium. This is believed to be induced by the X-ray beam during the measurement. The magnitude of this signal ranged from 20 to 35% of the total europium signal for the Eu_2O_3/TiO_2, Ti/Eu = 20, and Ti/Eu = 100 samples, respectively. This was in fact inspected as a function of X-ray irradiation time, and a proportional trend was observed. Due to the low concentration of the lanthanide ions, low irradiation exposures did not yield satisfactory signal-to-noise ratios. The XPS analysis of the Yb_2O_3/TiO_2 catalyst reveals a signal at approximately 185.5 eV due to Yb^{3+} (4d) with a Ti/Yb = 200 ± 50. In the case of the Pr_2O_3/TiO_2 catalyst, the signal due to Pr^{3+} (3d) appears at 933.5 eV. The $Yb_2O_3/TiO_2$and Pr_2O_3/TiO_2 catalysts show a lower surface concentration of Ln^{3+} ions as compared to the concentration used in the preparation of the gel.

The photodegradation of salicylic acid and *t*-cinnamic acid by Eu_2O_3/TiO_2 was examined and compared with the nonmodified TiO_2. Figure 1 shows the absorbance spectra of salicylic acid solution at time intervals of irradiation with the Eu_2O_3/TiO_2 catalyst (Ti/Eu = 20). A substantial decrease in the absorbance of the substrate at all wavelengths is observed indicating its degradation. The substrate is completely degraded in the presence of the Eu_2O_3/TiO_2 catalyst. The absorbance spectra of salicylic acid reacted over Eu_2O_3/TiO_2 (Ti/Eu = 100), Pr_2O_3/TiO_2, and Yb_2O_3/TiO_2 catalysts after 60 min of irradiation were similar to of the Eu_2O_3/TiO_2 catalyst (Ti/Eu = 20), indicating its mineralization. In contrast, a smaller decrease ($\sim$54%) in the absorbance of the substrate is observed over the nonmodified TiO_2 catalyst after 60 min of irradiation (not shown). The photodegradation of salicylic acid by the lanthanide oxide doped TiO_2 catalysts leads

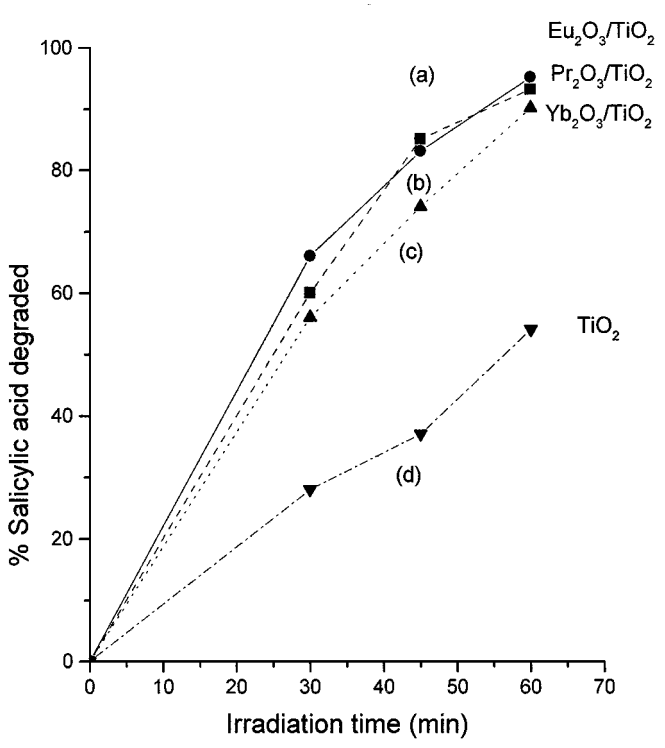

FIG. 2. Degradation of salicylic acid (2.4×10^{-4} M) over (a) Eu_2O_3/TiO_2 (Ti/Eu = 100) catalyst, (b) Pr_2O_3/TiO_2 catalyst, (c) Yb_2O_3/TiO_2 catalyst, and (d) nonmodified TiO_2 catalyst. In all experiments, 2.2–2.5 mg of the catalyst in 2.5 ml of the solution was used.

to complete mineralization as observed by GC–MS results (see later). The superior performance of the lanthanide oxide doped catalysts is clearly evident. Figure 2 shows the results obtained from the degradation of salicylic acid over the various TiO_2 catalysts. After 60 min of irradiation, 84, 95, 90, and 93% of salicylic acid are degraded by the Eu_2O_3/TiO_2 (Ti/Eu = 20),Eu_2O_3/TiO_2(Ti/Eu = 100), Pr_2O_3/TiO_2, and Yb_2O_3/TiO_2 catalysts as compared to 54% by the nonmodified TiO_2 photocatalyst.

To account for the enhanced photocatalytic activity of the lanthanide oxide doped catalysts as compared to the nonmodified TiO_2, the adsorption of salicylic acid to the Eu_2O_3/TiO_2 (Ti/Eu = 20) catalyst and nonmodified TiO_2 catalyst was examined. Figure 3 shows the adsorption isotherm of salicylic acid on Eu_2O_3/TiO_2 (Ti/Eu = 20). The amount of salicylic acid adsorbed onto the photocatalyst increases as the bulk concentration of the substrate is increased and then reaches a saturation value that represents the maximum loading of the substrate. For Eu_2O_3/TiO_2 (Ti/Eu = 20), the saturation value of 2.2×10^{-6} mol g^{-1} of salicylic acid on the catalyst is obtained at a bulk concentration of 2.65×10^{-3} M. The presence of an adsorption maximum indicates that a simple Langmuir equation, which assumes the presence of only one type of surface site, should be applicable in the present study. The adsorption isotherm was analyzed in terms of the Langmuir theory(35). A linear relationship in agreement with the Langmuir theory between $[C]_{eq}/C_{ads}$ as a function of $[C]_{eq}$ was obtained (not shown); $[C]_{eq}$ represents the equilibrium bulk concentration of salicylic acid and C_{ads} is the amount (in moles) of salicylic acid adsorbed onto the photocatalysts. Thus, a simple Langmuir equation did fit our data satisfactorily. This is in contrast to the results obtained by Tunesi and Anderson (24) and Regazzoni *et al.* (26). Tunesi and Anderson (24) reported a Freundlich isotherm to be a representation for the adsorption of salicylic acid and 3-chlorosalicylic acid over TiO_2 catalysts. They did not observe any adsorption maximum which may mean that they have not saturated the surface sites, or possibly have several types of sites or have a continuum of sites. A multisite surface complex model was proposed by Regazzoni *et al.* (26) to explain the adsorption of salicylic acid over the TiO_2 catalyst (Degussa P-25). Our results are in agreement with those reported by Cunningham and Al-Sayyed (36). This suggests that in the present study, the Ln_2O_3/TiO_2 composite photocatalysts consist of lanthanide oxide particles uniformly dispersed on the surface and in the bulk giving rise to TiO_2 surface hydroxyl groups that have only one degree of acidity. Thus, the surface with respect to the adsorption process is homogeneous accounting for the good fit to the one-site Langmuir adsorption isotherm. The derived adsorption constant on Eu_2O_3/TiO_2 (Ti/Eu = 20) is $K_{ads} = 4.08 \times 10^3$ M^{-1}. From Fig. 4 for the nonmodified TiO_2 catalyst, the saturation

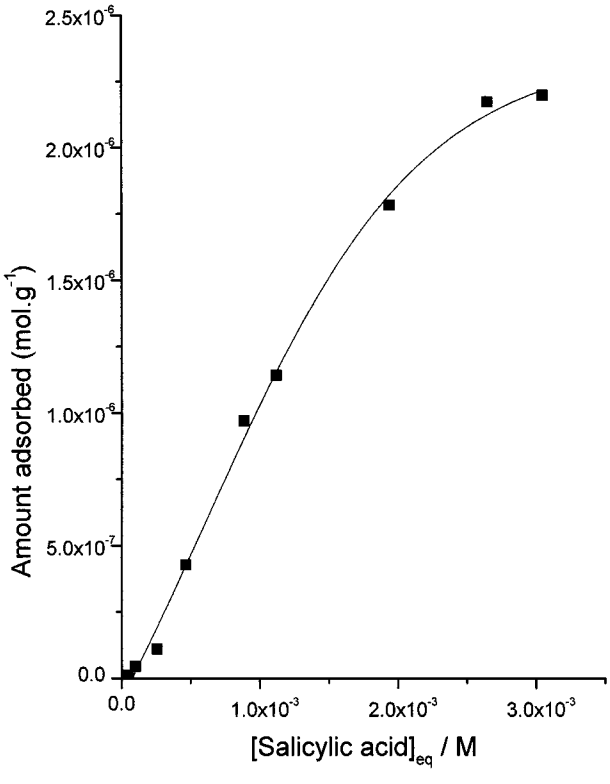

FIG. 3. Adsorption isotherm of salicylic acid over Eu_2O_3/TiO_2 catalyst (Ti/Eu = 20).

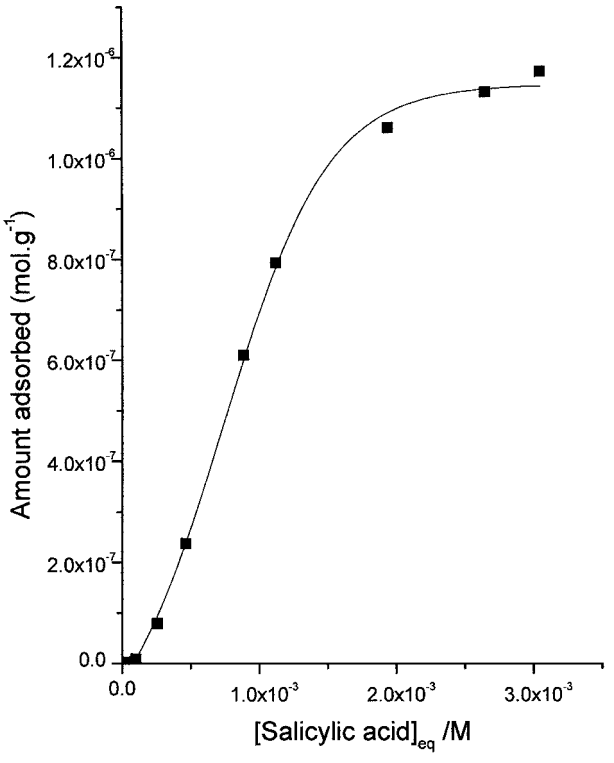

FIG. 4. Adsorption isotherm of salicylic acid over nonmodified TiO_2 catalyst.

value of 1.33×10^{-6} mol g^{-1} on the catalyst is obtained at a bulk concentration of 3.05×10^{-3} M. The derived adsorption constant on nonmodified TiO_2 is $K_{ads} = 1.25 \times 10^3$ M^{-1}. Similarly, the adsorption constants of salicylic acid were determined to be $K_{ads} = 3.6 \times 10^3$ M^{-1} for Eu_2O_3/TiO_2 (Ti/Eu = 100) $K_{ads} = 3.0 \times 10^3$ M^{-1} for Pr_2O_3/TiO_2, and $K_{ads} = 2.8 \times 10^3$ M^{-1} for Yb_2O_3/TiO_2. The enhanced adsorption constant is attributed to the formation of Lewis acid–base complexes between the lanthanide ions in the modified TiO_2 and the carboxylic acid residue of the substrate. The concentration of the substrate at the photocatalytic surface could then provide the mechanism for the enhanced mineralization of salicylic acid by the modified photocatalysts.

The concentrations of the solutions after irradiation were also monitored by GC–MS analyses. Table 2 shows the results obtained from the GC–MS study for the degradation of salicylic acid by the lanthanide oxide doped catalysts. The GC–MS results clearly reveal the superior performance of the lanthanide oxide doped catalysts. For example, from Table 2 we can see that after 30 min of irradiation, the concentration of salicylic acid is 11.2 ppm with the Eu_2O_3/TiO_2 catalyst (Ti/Eu = 100), whereas it is 25.5 ppm with the nonmodified catalyst. After 60 min of irradiation, complete mineralization of salicylic acid is achieved by the lanthanide oxide doped catalysts while the concentration of salicylic acid is 17.4 ppm with the nonmodified catalyst. The spectroscopic assay of the degradation rates of salicylic acid coincides with the results obtained from the GC–MS analysis of the irradiated samples. Figure 5 shows the results obtained from the GC–MS analysis and the spectroscopic analysis for the Eu_2O_3/TiO_2 catalyst (Ti/Eu = 100).

It is worthwhile to also compare the rate of photodegradation of salicylic acid by Eu_2O_3/TiO_2 catalysts that include different amounts of europium oxide. The rate of degradation of salicylic acid was found to be twice as fast in the presence of the Eu_2O_3/TiO_2 catalyst (Ti/Eu = 100) ($k = 2.2$ s^{-1}) as compared to the photocatalyst containing Ti/Eu = 20 ($k = 0.9$ s^{-1}). The rate of degradation was estimated from the initial decrease in the concentration of salicylic acid assuming first-order kinetics. The fact that the Eu_2O_3/TiO_2 catalyst (Ti/Eu = 20) is less efficient implies that the improved adsorption of the pollutants to the europium oxide doped photocatalysts is not the sole operative mechanism that controls the activity of the photocatalysts since the adsorption of salicylic acid is higher on the Ti/Eu catalyst (Ti/Eu = 20) ($K_{ads} = 4.08 \times 10^3$ M^{-1}) compared to the Eu_2O_3/TiO_2 catalyst (Ti/Eu = 100) ($K_{ads} = 3.6 \times 10^3$ M^{-1}). The Eu_2O_3/TiO_2 catalyst (Ti/Eu = 20) absorbs ca. 20% more incident light as compared to the Ti/Eu = 100 catalyst (not shown). Thus the lower activity exhibited by

TABLE 2

GC–MS Results Obtained for the Degradation of Salicylic Acid over Lanthanide Oxide Doped TiO_2 Catalysts and Nonmodified TiO_2 Catalyst

	TiO_2		Eu_2O_3/TiO_2 (Ti/Eu = 100)		Pr_2O_3/TiO_2		Yb_2O_3/TiO_2	
Time (min)	GC–FID/MS (ppm)	DOC (ppm)	GC–FID/MS (ppm)	DOC (ppm)	GC–FID/MS (ppm)	DOC (ppm)	GC–FID/MS (ppm)	DOC (ppm)
0	33.9	34.5	33.9	34.5	33.9	34.5	33.9	34.5
15	30.8	35.0	n.d.[a]	n.d.	n.d.	n.d.	n.d.	n.d.
30	25.5	32.5	11.2	17.2	14.9	24.8	13.5	21.5
45	n.d.	n.d.	5.5	8.4	8.8	16.1	5.0	11.1
60	17.4	26.0	0.0	1.5	0.0	2.2	0.5	4.1

[a] Not determined.

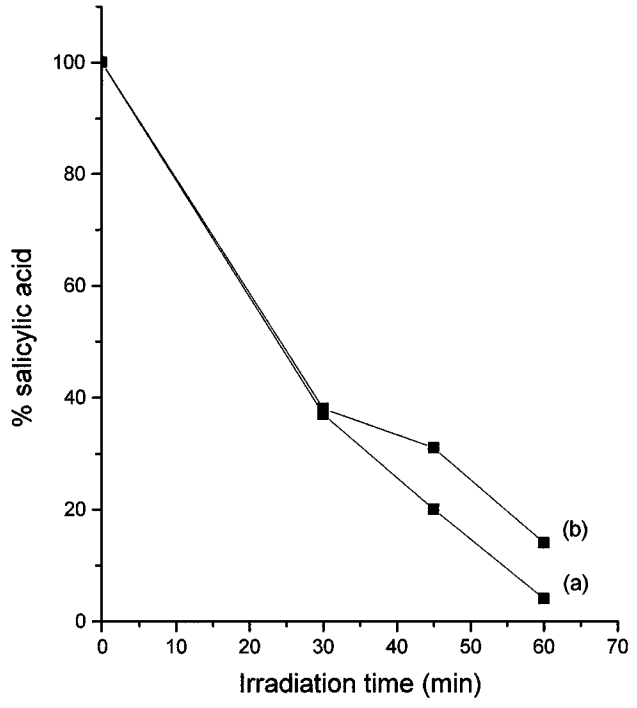

FIG. 5. Degradation of salicylic acid (2.4×10^{-4} M) over Eu_2O_3/TiO_2 (Ti/Eu = 100) catalyst (a) analyzed by GC–MS, (b) analyzed spectroscopically. In all experiments, 2.2–2.5 mg of the catalyst in 2.5 ml of the solution was used.

the Eu_2O_3/TiO_2 catalyst (Ti/Eu = 20) can be attributed to the light filtering effect since europium oxide absorbs part of the incident light. The onset of absorption for Eu_2O_3 is ~320 nm.

In order to test the generality of the enhanced activity of the lanthanide oxide doped catalysts, the degradation of another aromatic carboxylic acid compound, namely, *t*-cinnamic acid, was evaluated. Figure 6 shows the absorption spectra of *t*-cinnamic acid solution at time intervals of irradiation with the lanthanide oxide doped catalysts and the nonmodified TiO_2 catalyst. It is evident that the substrate is degraded at an impressive rate in the presence of the lanthanide oxide doped catalysts as compared to the nonmodified TiO_2 catalyst. *t*-cinnamic acid is completely degraded in the presence of the lanthanide oxide doped catalysts after 60 min of irradiation whereas only 45% is degraded by the nonmodified TiO_2 catalyst (Fig. 7). Table 3 summarizes the results obtained from the photodegradation of salicylic acid and *t*-cinnamic acid over nonmodified TiO_2 and Ln_2O_3/TiO_2 photocatalysts. Table 4 shows the results obtained from the GC–MS analyses. The GC–MS results indicate that *t*-cinnamic acid is completely degraded

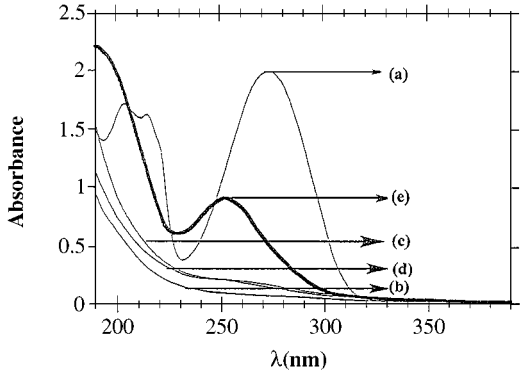

FIG. 6. Absorption spectra of an aqueous solution of *t*-cinnamic acid (2.2×10^{-5} M) (a) before irradiation, (b) after 45 min of irradiation in the presence of the Eu_2O_3/TiO_2 (Ti/Eu = 100) catalyst, (c) after 45 min of irradiation in the presence of the Pr_2O_3/TiO_2 (Ti/Pr = 100) catalyst, (d) after 45 min of irradiation in the presence of the Yb_2O_3/TiO_2 (Ti/Yb = 100) catalyst, and (e) after 45 min of irradiation in the presence of the nonmodified TiO_2 catalyst. In all experiments, 2.2–2.5 mg of the catalyst in 2.5 ml of the solution was used.

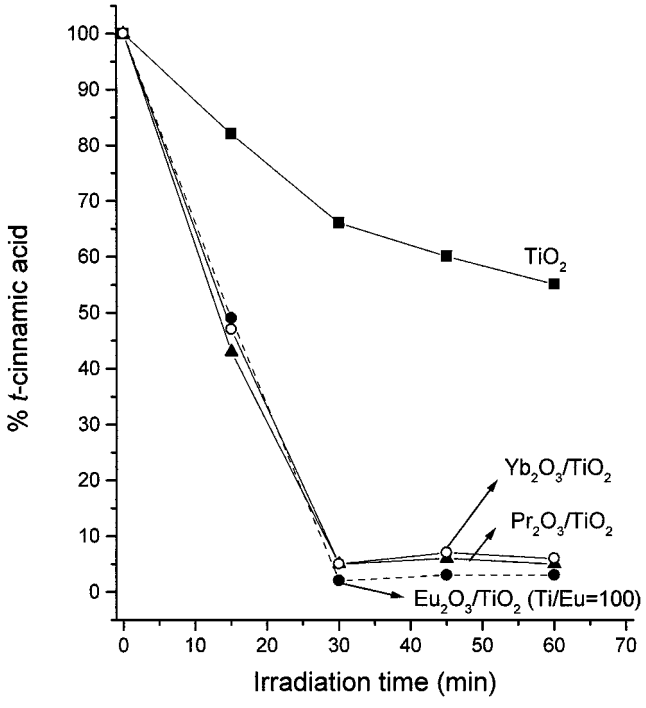

FIG. 7. Degradation of *t*-cinnamic acid (2.2×10^{-5} M) over Ln_2O_3/TiO_2 catalysts and nonmodified TiO_2 catalyst.

TABLE 3

Amount of Salicylic Acid and *t*-Cinnamic Acid Degraded (Analyzed Spectroscopically) after 60 and 45 min of Irradiation over Lanthanide Oxide Doped TiO_2 Catalysts and Nonmodified TiO_2 Catalyst, Respectively

Catalyst	Salicylic acid degraded (%)	*t*-Cinnamic acid degraded (%)
TiO_2	54[a]	45[a]
Eu_2O_3/TiO_2 (Ti/Eu = 20)	84	90
Eu_2O_3/TiO_2 (Ti/Eu = 100)	95	98
Pr_2O_3/TiO_2	90	95
Yb_2O_3/TiO_2	93	95

[a] Formation of intermediates.

TABLE 4

GC–MS Results Obtained for the Degradation of *t*-Cinnamic Acid over Lanthanide Oxide Doped TiO_2 Catalysts and Nonmodified TiO_2 Catalyst

	TiO_2		Eu_2O_3/TiO_2 (Ti/Eu = 100)		Pr_2O_3/TiO_2		Yb_2O_3/TiO_2	
Time (min)	GC–FID/MS (ppm)	DOC (ppm)	GC–FID/MS (ppm)	DOC (ppm)	GC–FID/MS (ppm)	DOC (ppm)	GC–FID/MS (ppm)	DOC (ppm)
0	58.0	58.0	58.0	58.0	58.0	58.0	58.0	58.0
15	51.2	56.5	24.0	40.2	18.7	35.0	28.5	41.5
30	38.4	51.4	0.0	18.7	0.0	4.9	5.6	20.3
45	31.6	45.0	0.0	9.5	0.0	1.1	0.0	12.7

in the presence of Eu_2O_3/TiO_2 and Pr_2O_3/TiO_2 catalysts after 30 min of irradiation, whereas only 34% is degraded over the nonmodified TiO_2 catalyst. After 45 min of irradiation, complete degradation of *t*-cinnamic acid is achieved by Ln_2O_3/TiO_2 photocatalysts, whereas 45% is degraded by the nonmodified TiO_2 photocatalyst. The GC–MS results indicate that in the case of the nonmodified TiO_2 catalyst at least 20 intermediates were detected. Some of the intermediates that were detected were phenol, oxalic acid, salicylic acid, and benzoic acid. For Ln_2O_3/TiO_2 photocatalysts, oxalic acid was detected as the only intermediate. After 45 min of irradiation, the concentration of oxalic acid was found to be 2.7 ppm for Eu_2O_3/TiO_2, 1.0 ppm for Yb_2O_3/TiO_2, and 2.5 ppm for Pr_2O_3/TiO_2.

The adsorption constants of *t*-cinnamic acid over the lanthanide oxide doped catalysts and the nonmodified TiO_2 catalyst were evaluated. The adsorption constants were determined to be $K_{ads} = 6.0 \times 10^2\ M^{-1}$ for nonmodified TiO_2, $K_{ads} = 2.0 \times 10^3\ M^{-1}$ for Eu_2O_3/TiO_2 (Ti/Eu = 100), $K_{ads} = 1.5 \times 10^3\ M^{-1}$ for Pr_2O_3/TiO_2, and $K_{ads} = 1.2 \times 10^3\ M^{-1}$ for Yb_2O_3/TiO_2. The adsorption isotherms could be fitted by a simple Langmuir equation.

The discussion henceforth pertains to the factors leading to the enhanced activity of the lanthanide oxide doped TiO_2 catalysts. The crystalline phase of the titania catalyst is an important factor that determines its activity. The lanthanide oxide containing catalysts exist predominantly in the anatase phase, whereas the nonmodified TiO_2 catalyst contains 20% of rutile phase. One possible reason for the decrease in activity of the nonmodified TiO_2 particles could be the presence of the rutile phase. The phase change from anatase to rutile occurs in the temperature range of 600–1100°C. It has been suggested by Ovenstone and Yanagisawa (37) that a critical particle size is required for the anatase to rutile transformation. The critical particle size required for rutile formation is larger than the normal anatase crystallite size for a sol-produced powder. The presence of lanthanide oxide particles in the composite Ln_2O_3/TiO_2 photocatalysts prevents anatase particles from adhering together and thus a critical particle size necessary for the transformation from anatase to rutile is prevented. The significant differences obtained in the activities cannot be attributed to the differences in the phase composition alone.

Another factor that could greatly influence the photocatalytic activity is the surface area of the catalysts. The surface areas of Eu_2O_3/TiO_2 and PrO_3/TiO_2 are similar (102.1 $m^2\ g^{-1}$ and 125.0 $m^2\ g^{-1}$, respectively) while that of Yb_2O_3/TiO_2 is about 25% lower than that of Eu_2O_3/TiO_2. The surface area of the nonmodified TiO_2 is 78.1 $m^2\ g^{-1}$. The photocatalytic activity of Yb_2O_3/TiO_2 is comparable to the other lanthanide oxide doped catalysts, suggesting that the differences in the surface area cannot be a controlling factor in influencing the photocatalytic activity.

The particles in the composite photocatalysts consist of lanthanide oxides and TiO_2 particles. The formation of a heterojunction between TiO_2 and Ln_2O_3 could prevent electron–hole recombination and enhance the activity. However, the conduction band edges of lanthanide oxides lie at far more negative values (∼−1.8 to −3.5 V vs standard hydrogen electrode (SHE) compared to TiO_2(∼−0.3 V vs SHE for anatase). Hence, electron transfer is not possible from the conduction band edge of TiO_2 to Ln_2O_3 since the lanthanide oxides do not possess the appropriate potentials. Thus, the formation of such heterojunctions cannot explain the enhanced activity by Ln_2O_3/TiO_2 photocatalysts.

The adsorption of salicylic acid and that of *t*-cinnamic acid were found to be ca. three times and two times higher, respectively, on the lanthanide oxide modified catalysts compared to the nonmodified TiO_2 catalyst. This would suggest that the equilibrium dark adsorption of the pollutant at the photocatalyst surface has an important role in determining the photocatalytic activity. The lanthanide oxide doped TiO_2 catalysts turned bright yellow upon immersion in salicylic acid solutions, whereas the nonmodified TiO_2 catalyst turned pale yellow. The supernatant solutions were, however, colorless. The development of a bright yellow color is a clear indication of the formation of Lewis acid–base complexes between the lanthanide ions and the carboxylic acid residues of the substrate. Complexes between the

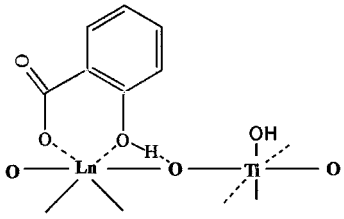

SCHEME 2. Surface complex formed between salicylic acid and Ln_2O_3/TiO_2 catalysts.

substrates and pure TiO_2 can also be formed. The equilibrium constant for the formation of Ti^{4+}–salicylic acid is estimated to be $K = 2.2 \times 10^2$ (38) and for Ln^{3+}–salicylic acid ($Ln = Eu^{3+}$, Pr^{3+}), $K = 5.0 \times 10^2$ (39). Thus, the relative tendency for the formation of surface complexes of the type described in Scheme 2 is higher for Ln^{3+} compared to Ti^{4+}. The concentration of the pollutant at the photocatalyst could provide the mechanism for the enhanced mineralization by the modified catalysts. We interpret our enhanced adsorption of salicylic acid due to the formation of surface complexes as described in Scheme 2. The adsorption of *t*-cinnamic acid over the lanthanide oxide doped TiO_2 catalysts was found to be lower when compared with salicylic acid. The lower adsorption for *t*-cinnamic acid can be explained by considering that it does not have the appropriate stereochemical configuration to make ring formation possible as in salicylic acid. Thus the behavior of *t*-cinnamic acid lends credence to our suggested structure of the surface complex.

An enhancement of the activity would also occur if the surface complex between the lanthanide ions and the organic acid is photoactive and helps in a charge transfer reaction.

The photocatalytic oxidation involves multiple steps. The identification of intermediates depends on the stability of the intermediates themselves as most of them undergo rapid oxidation. In the present work, in the case of lanthanide oxide doped TiO_2 catalysts, oxalic acid was detected as the *only* intermediate. The formation of oxalic acid as the only intermediate indicates the degradation route to complete mineralization of the substrates to CO_2. The exact reason for the formation of only oxalic acid in solution is unclear at the moment since oxalic acid too has a tendency to bind to the lanthanide ions. In the case of the nonmodified TiO_2 catalyst, the photodegradation is slow and incomplete. Twenty intermediates were observed but their concentrations were too low to be quantitatively estimated.

In conclusion, we have designed a new class of photocatalysts for the degradation of functionalized aromatic acids. The photocatalysts consist of lanthanide oxide/TiO_2 composites. The present study has demonstrated that europium, praseodymium, and ytterbium oxide doped TiO_2 exhibit significantly higher activity compared to the nonmodified TiO_2 catalyst. The enhanced degradation by the lanthanide oxide doped TiO_2 is thus general, and other organic compounds such as *p*-chlorophenoxyacetic acid, *p*-nitrobenzoic acid, and aniline can be completely mineralized. Since the photodegradation involves oxidative mineralization, the intermediates are bound to the lanthanide ions and their surface degradation prevents their appearance in solution. The loading of the lanthanide ions is also an important parameter.

ACKNOWLEDGMENTS

This research was supported by the Israel Ministry of Science (MOS), Israel, and the Bundesministerium für Bilding, Wissenschaft, Forschung und Technologie (BMBF), Germany.

REFERENCES

1. Legrini, O., Oliveros, E., and Braun, A. M., *Chem. Rev*. **93**, 671 (1993).
2. Hoffmann, M. R., Martin, S. T., Choi, W., and Bahnemann, D. W., *Chem. Rev*. **95**, 69 (1995).
3. Bahnemann, D. W., *Res. Chem. Intermed*. **26**, 207 (2000).
4. Litter, M. I., *Appl. Catal. B Environ*. **23**, 89 (1999).
5. Blake, D. M., "Bibliography of Work on the Photocatalytic Removal of Hazardous Compounds from Water and Air." NREL/TP-340-22197, National Renewable Energy Laboratory, Golden, CO, 1997.
6. Mills, G., and Hoffmann, M. R., *Environ. Sci. Technol*. **27**, 1681 (1993).
7. Mas, D., Delprat, H., and Pichat, P., *Proc. Electrochem. Soc*. **97**, 289 (1997).
8. Gonzalez-Martin, A., and Sidik, R. A., *Proc. Electrochem. Soc*. **98**, 193 (1998).
9. Kisch, H., Zang, L., Lange, C., Maier, W. F., Wilhelm, F., Antonius, C., and Meissner, D., *Angew. Chem. Int. Ed*. **37**, 3034 (1998).
10. Xu, N., Shi, Z., Fan, Y., Dong, J., Shi, J., and Hu, M. Z.-C., *Ind. Eng. Chem. Res*. **38**, 373 (1999).
11. Borgarello, E., Serpone, N., Emo, G., Harris, R., Pelizzetti, E., and Minero, C., *Inorg. Chem*. **25**, 4499 (1986).
12. Ollis, D. F., Pelizzetti, E., and Serpone, N., *Environ. Sci. Technol*. **25**, 1523 (1991).
13. Albert, M., Gao, Y. M., Toft, D., Dwight, K., and Wold, A., *Mater. Res. Bull*. **27**, 961 (1992).
14. Inel, Y., and Ertek, D., *J. Chem. Soc., Faraday. Trans*. **89**, 129 (1993).
15. Willner, I., Eichen, Y., and Frank, A. J., *J. Am. Chem. Soc*. **111**, 1884 (1989).
16. Nakahira, T., and Grätzel, M., *J. Phys. Chem*. **88**, 4006 (1984).
17. Frank, A. J., Willner, I., Goren, Z., and Degani, Y., *J. Am. Chem. Soc*. **109**, 3568 (1987).
18. Ranjit, K. T., Cohen, H., Willner, I., Bossmann, S., and Braun, A. M., *J. Mater. Sci*. **34**, 5273 (1999).
19. Mao, Y., Schoneich, C., and Asmus, K. D., *J. Phys. Chem*. **95**, 80 (1991).
20. Ranjit, K. T., Joselevich, E., and Willner, I., *J. Photochem. Photobiol., A Chem*. **96**, 185 (1996).
21. Rabenstein, D. L., *Anal. Chem*. **43**, 1599 (1971).
22. Brinker, C. J., and Scherer, G. W., "The Physics and Chemistry of Sol-Gel Processing." Academic Press, New York, 1990.
23. Ranjit, K. T., Willner, I., Bossmann, S., and Braun, A. M., *Environ. Sci. Technol*. **35**, 1544 (2001).
24. Tunesi, S., and Anderson, M. A., *J. Phys. Chem*. **95**, 3399 (1991).
25. Moser, J., Punchihewa, S., Infelta, P. P., and Grätzel, M., *Langmuir* **7**, 3012 (1991).
26. Regazzoni, A. E., Mandelbaum, P., Matsuyoshi, M., Schiller, S., Bilmes, S. A., and Blesa, M. A., *Langmuir* **14**, 868 (1998).
27. Matthews, R. W., *J. Catal*. **111**, 264 (1988).

28. Matthews, R. W., *J. Phys. Chem*. **91**, 3328 (1987).
29. Matthews, R. W., *Aust. J. Chem*. **40**, 667 (1987).
30. Matthews, R. W., and McEvoy, S. R., *J. Photochem. Photobiol., A Chem*. **66**, 355 (1992).
31. Matthews, R. W., *Water Res*. **24**, 653 (1990).
32. Dagan, G., and Tomkiewicz, M., *in* "Proceedings, Electrochemical Society, 93-18, Proceedings of the Symposium on Environmental Aspects of Electrochemistry and Photoelectrochemistry, 1993," p. 137. Honolulu, HI, 1993.
33. Dagan, G., and Tomkiewicz, M., *J. Phys. Chem*. **97**, 12,651 (1993).
34. Lakshmi, B. B., and Martin, C. R., *in* "Proceedings of Electrochemistry Society, 97-11, Quantum Confinement: Nanoscale Materials, Devices and Systems, 1997," p. 47. Quebec, Canada, 1997.
35. Langmuir, I., *J. Am. Chem. Soc*. **40**, 1361 (1918).
36. Cunningham, J., and Al-Sayyed, G., *J. Chem. Soc., Faraday Trans*. **86**, 3935 (1990).
37. Ovenstone, J., and Yanagisawa, K., *Chem. Mater*. **11**, 2770 (1999).
38. Hultquist, A. E., *Anal. Chem*. **36**, 149 (1964).
39. Sinha, S. P., "Complexes of the Rare Earths." Pergamon, New York, 1966.